Bidirectional Hybrid Quantum Communication of Two-Qubit States

Yao Lu 陆尧 [1], Min Jiang 姜敏 [2,*]

[1]School of Electronics and Information Engineering,
Soochow University, Soochow, China

[2]School of Electronics and Information Engineering,
Soochow University, Soochow, China

2026 年 8 月 16 日

Abstract

This paper proposes a hybrid bidirectional quantum communication protocol, in which two parties simultaneously transmit two-qubit states: one via quantum teleportation (QT) and the other via remote state preparation (RSP). This approach establishes a more flexible model for bidirectional quantum communication. The protocol utilizes a specially designed maximally entangled quantum channel to enable hybrid bidirectional communication. By performing Bell measurements, joint projective measurements, and corresponding unitary operations, quantum teleportation from Alice to Bob and remote state preparation from Bob to Alice can be accomplished synchronously. Furthermore, the robustness of the proposed protocol is evaluated under three typical noisy environments, namely the amplitude damping (AD) channel, phase damping(PD) channel and the depolarizing (DP) channel. The proposed protocol provides a novel framework for efficient bidirectional quantum communication, with potential advantages in enhancing interactivity and optimizing resource utilization in future quantum networks.

Keywords: Bidirectional quantum communication, Quantum teleportation, Remote state preparation, Two-qubit state

PACS: 03.67.-a, 03.67.Hk, 03.67.Mn

1. Introduction

Over the past two decades, quantum mechanics, information science, and computer science have undergone rapid development and become increasingly intertwined. Quantum entanglement is a fundamental phenomenon in which the states of two or more particles become correlated, independent of the distance between them. This correlation is independent of the distance between the particles and represents a form of non-local correlation. It provides the foundation for many quantum information protocols, the

*∗ Min Jiang 姜敏. E-mail: jiangmin08@suda.edu.cn

most representative of which is quantum teleportation (QT). Bennett et al. proposed the first Quantum Teleportation (QT) protocol in 1993, which enabled a sender to transmit an unknown quantum state to a distant receiver through the use of classical communication and one pre-shared Einstein–Podolsky–Rosen (EPR) entangled pair.QT enables the transfer of an unknown quantum state from one location to another without physically transmitting the associated particle, by consuming two classical bits of information and a shared entangled Bell state. This protocol relies on the shared entangled state between the sender and receiver, as well as classical communication. It holds profound implications for secure quantum communication, enabling long-distance transmission of quantum information and supporting the development of quantum networks.

While QT transmits unknown quantum states, Remote State Preparation (RSP) [2] aims to prepare a known state at a distant location, using shared entanglement and classical communication, without physically transmitting the quantum system itself. RSP was also first proposed by Bennett et al. with the goal of improving communication efficiency and reducing the cost as well as resource consumption, which played a vital role in applications such as distributed quantum computing and quantum cryptography. By combining entanglement resources with classical communication, RSP enables the manipulation of quantum information at spatially separated nodes, thereby establishing itself as a core technology for future quantum networks. This approach opens up promising research avenues for enhancing the scalability and reliability of quantum communication infrastructures.

To meet the diverse needs of quantum communication in various scenarios, several variants of QT and RSP have been developed, including Controlled Quantum Teleportation (CQT), Joint Remote State Preparation (JRSP), and Deterministic Remote State Preparation (DRSP), which enhance security, collaboration, and determinism in quantum transmission. Among these, Bidirectional Quantum State Teleportation (BQST) has emerged as a key paradigm, enabling two parties to simultaneously and independently transmit unknown quantum states. It is of great significance for improving the communication efficiency of quantum networks and enabling bidirectional interactive control, and it has become an important branch in the study of quantum communication. Early studies mainly focused on BQST and simple entangled resources. For example, Kazemikhah et al. [13] proposed an asymmetric bidirectional controlled QT scheme using an eight-qubit cluster state, achieving efficient and secure asymmetric transmission of two- and three-qubit states. Wang and Li [15] used a five-qubit cluster state for asymmetric transmission between a two-qubit EPR pair and a single-qubit state, optimizing efficiency and reducing classical resource usage with local CNOT operations. More recently, Yuan et al. [16] introduced a bidirectional quantum operation teleportation protocol based on two four-qubit cluster states, allowing remote users to perform single-qubit operations on each other’ s target states, with advantages in determinism, efficiency, and experimental feasibility.

This paper presents a novel controlled hybrid bidirectional quantum communication protocol for two-qubit states. By integrating quantum teleportation (QT) for unknown state transmission and remote state preparation (RSP) for known state preparation within a single framework, the proposed scheme

breaks the boundary of conventional single-mechanism bidirectional protocols, enabling asynchronous yet synchronous bidirectional quantum information exchange.

To support this hybrid architecture, a specially designed 11-qubit maximally entangled quantum channel is constructed, which effectively decouples the QT and RSP subsystems to eliminate cross-talk and mutual quantum interference during parallel execution. Meanwhile, a third-party controller (TP) provides deterministic operational control over the entire transmission process, guaranteeing a 100% theoretical success rate under ideal conditions. Furthermore, to evaluate practical feasibility, we systematically investigate the protocol's robustness across three representative noisy environments—amplitude damping (AD), phase damping (PD), and depolarizing (DP) channels—under a single-sided noise model that mimics asymmetric physical setups. Theoretical evaluations demonstrate the operational viability of the scheme under realistic weak decoherence, while highlighting the distinct phase sensitivity of the RSP subsystem to guide future error mitigation strategies. The proposed scheme achieves a favorable balance between entanglement resources and functional versatility, providing a scalable and flexible building block for future heterogeneous quantum networks.

2. Bidirectional Hybrid Transmission of Two-qubit States

Here we present a hybrid scheme for a two-qubit quantum communication system consisting of QT of an unknown state and RSP of a known state under ideal conditions.

The protocol involves three participants: Alice, Bob, and a third-party controller TP. Let's ignore the global factors. The entanglement channel shared by Alice, Bob and TP is in the following form

$$\begin{aligned}|\zeta\rangle =&\frac{1}{4\sqrt{2}}\Big[(|00\rangle+|11\rangle)_{12}(|00\rangle+|11\rangle)_{34}(|000\rangle+|111\rangle)_{567}(|000\rangle+|111\rangle)_{8910}|0\rangle_{11}\\&+(|00\rangle-|11\rangle)_{12}(|00\rangle-|11\rangle)_{34}(|000\rangle-|111\rangle)_{567}(|000\rangle-|111\rangle)_{8910}|1\rangle_{11}\Big]\end{aligned} \tag{1}$$

The distribution of particles among the parties is illustrated in Figure 1. Alice holds particles 1, 3, 7, 10; while Bob holds particles 2, 4, 5, 6, 8, 9; and TP holds particle 11.

The QT subsystem consists of particles 1, 2, 3, and 4, while the RSP subsystem consists of particles 5, 6, 7, 8, 9, and 10.

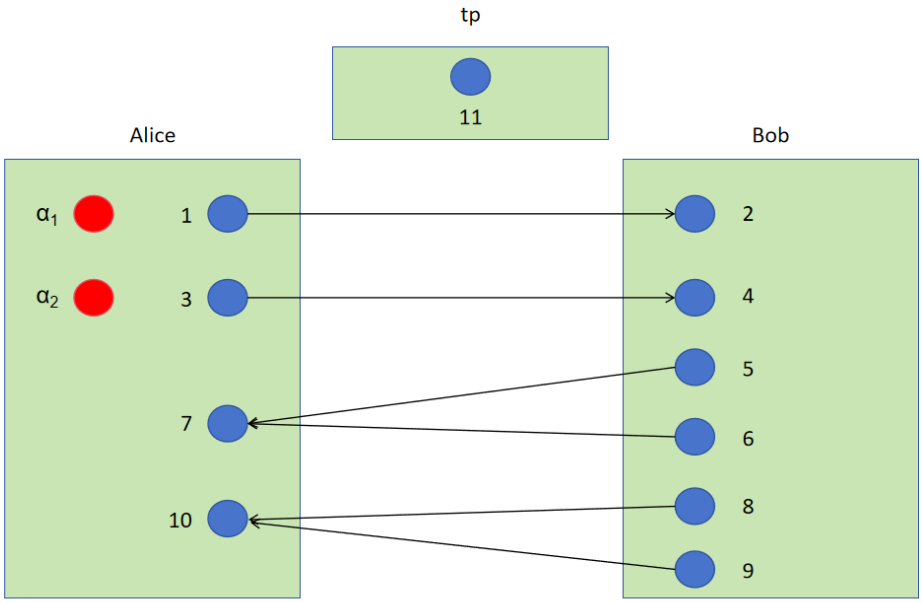


Fig. 1. The two-qubit bidirectional communication protocol.

In this scheme, quantum information is transmitted from Alice to Bob via QT, and from Bob to Alice via RSP. The unknown state to be held by Alice $|\varepsilon\rangle$ is defined as follows

$$|\varepsilon\rangle_{\alpha_1\alpha_2} = (a_0|00\rangle + a_1|01\rangle + a_2|10\rangle + a_3|11\rangle)_{\alpha_1\alpha_2} \tag{2}$$

where a_i are unknown and they satisfy the normalization conditions $|a_0|^2 + |a_1|^2 + |a_2|^2 + |a_3|^2 = 1$.

The state to be prepared by Bob $|\varphi\rangle$ is given by

$$|\varphi\rangle = b_0\,|00\rangle + b_1 e^{i\lambda_1}\,|01\rangle + b_2 e^{i\lambda_2}\,|10\rangle + b_3 e^{i\lambda_3}\,|11\rangle \tag{3}$$

where b_i satisfy the normalization conditions $b_0^2 + b_1^2 + b_2^2 + b_3^2 = 1$ and $\lambda_i \in [0, 2\pi)$.

To complete the hybrid quantum communication of two-qubit states, the following steps are required. Now, turn to the QT subsystem from Alice to Bob. After receiving TP's measurement result, Alice performs Bell-state measurements (BSMs) on her two particle pairs $(a_1, 1)\,(a_2, 3)$. In the two-qubit case, the Bell measurement basis is given by

$$\begin{aligned} |\phi_{00}\rangle = \frac{1}{\sqrt{2}}\left(|00\rangle + |11\rangle\right), |\phi_{01}\rangle = \frac{1}{\sqrt{2}}\left(|01\rangle + |10\rangle\right), \\ |\phi_{10}\rangle = \frac{1}{\sqrt{2}}\left(|00\rangle - |11\rangle\right), |\phi_{11}\rangle = \frac{1}{\sqrt{2}}\left(|01\rangle - |10\rangle\right) \end{aligned} \tag{4}$$

If TP agrees to the quantum communication, then particle 11 will be measured by the two bases $|0\rangle_{11}$ and $|1\rangle_{11}$ and TP will report the measurement result to both Alice and Bob. Then Alice will apply CNOT gates on the two pairs of particles $(a_1, 1)\,(a_2, 3)$. Here, we assume that the measurement result of

the third-party TP particle is $|0\rangle_{11}$. Now, the state of the QT subsystem then becomes

$$\begin{aligned}
&|\zeta_1\rangle_{\alpha_1\alpha_2 1234} = \mathrm{CNOT}_{\alpha_1 1}\mathrm{CNOT}_{\alpha_2 3}\,|\zeta\rangle_{\alpha_1\alpha_2 1234} \\
&= \begin{pmatrix}
a_0\,|000000\rangle + a_0\,|000011\rangle + a_0\,|001100\rangle + a_0\,|001111\rangle \\
+a_1\,|010010\rangle + a_1\,|010001\rangle + a_1\,|011110\rangle + a_1\,|011101\rangle \\
+a_2\,|101000\rangle + a_2\,|101011\rangle + a_2\,|100100\rangle + a_2\,|100111\rangle \\
+a_3\,|111010\rangle + a_3\,|111001\rangle + a_3\,|110110\rangle + a_3\,|110101\rangle
\end{pmatrix}_{\alpha_1\alpha_2 1234}
\end{aligned} \tag{5}$$

Subsequently, Hadamard (H) operations are applied to the two particles $(a_1, 1)\,(a_2, 3)$ to complete the Bell-state measurement. Now, the state of QT subsystem can be written as

$$\begin{aligned}
&|\zeta_2\rangle_{\alpha_1\alpha_2 1234} = H_{\alpha_1}H_{\alpha_2}\,|\zeta_1\rangle_{\alpha_1\alpha_2 1234} \\
&= \{a_0\,[(|0\rangle + |1\rangle)\,(|0\rangle + |1\rangle)\,(|0000\rangle + |0011\rangle + |1100\rangle) + |1111\rangle] \\
&+ a_1\,[(|0\rangle + |1\rangle)\,(|0\rangle - |1\rangle)\,(|0010\rangle + |0001\rangle + |1110\rangle + |1101\rangle)] \\
&+ a_2\,[(|0\rangle - |1\rangle)\,(|0\rangle - |1\rangle)\,(|1000\rangle + |1011\rangle + |0100\rangle + |0111\rangle)] \\
&+ a_3\,[(|0\rangle - |1\rangle)\,(|0\rangle - |1\rangle)\,(|1010\rangle + |1001\rangle + |0110\rangle + |0101\rangle)]\}_{\alpha_1\alpha_2 1234}
\end{aligned} \tag{6}$$

By extracting particles 2 and 4 from the QT subsystem, the state to be teleported $|\varepsilon\rangle$ is obtained. In specific terms, the QT subsystem can be expressed as

$$|\zeta_3\rangle =$$

$$\begin{bmatrix}
|0000\rangle_{\alpha_1 1\alpha_2 3}(a_0|00\rangle + a_1|01\rangle + a_2|10\rangle + a_3|11\rangle)_{24} + |0001\rangle_{\alpha_1 1\alpha_2 3}(a_0|01\rangle + a_1|00\rangle + a_2|11\rangle + a_3|10\rangle)_{24} \\
+|0010\rangle_{\alpha_1 1\alpha_2 3}(a_0|10\rangle + a_1|11\rangle + a_2|00\rangle + a_3|01\rangle)_{24} + |0011\rangle_{\alpha_1 1\alpha_2 3}(a_0|11\rangle + a_1|10\rangle + a_2|01\rangle + a_3|00\rangle)_{24} \\
+|0100\rangle_{\alpha_1 1\alpha_2 3}(a_0|00\rangle - a_1|01\rangle + a_2|10\rangle - a_3|11\rangle)_{24} + |0101\rangle_{\alpha_1 1\alpha_2 3}(a_0|01\rangle - a_1|00\rangle + a_2|11\rangle - a_3|10\rangle)_{24} \\
+|0110\rangle_{\alpha_1 1\alpha_2 3}(a_0|10\rangle - a_1|11\rangle + a_2|00\rangle - a_3|01\rangle)_{24} + |0111\rangle_{\alpha_1 1\alpha_2 3}(a_0|11\rangle - a_1|10\rangle + a_2|01\rangle - a_3|00\rangle)_{24} \\
+|1000\rangle_{\alpha_1 1\alpha_2 3}(a_0|00\rangle + a_1|01\rangle - a_2|10\rangle - a_3|11\rangle)_{24} + |1001\rangle_{\alpha_1 1\alpha_2 3}(a_0|01\rangle + a_1|00\rangle - a_2|11\rangle - a_3|10\rangle)_{24} \\
+|1010\rangle_{\alpha_1 1\alpha_2 3}(a_0|10\rangle + a_1|11\rangle - a_2|00\rangle - a_3|01\rangle)_{24} + |1011\rangle_{\alpha_1 1\alpha_2 3}(a_0|11\rangle + a_1|10\rangle - a_2|01\rangle - a_3|00\rangle)_{24} \\
+|1100\rangle_{\alpha_1 1\alpha_2 3}(a_0|00\rangle - a_1|01\rangle - a_2|10\rangle + a_3|11\rangle)_{24} + |1101\rangle_{\alpha_1 1\alpha_2 3}(a_0|01\rangle + a_1|00\rangle - a_2|11\rangle - a_3|10\rangle)_{24} \\
+|1110\rangle_{\alpha_1 1\alpha_2 3}(a_0|10\rangle - a_1|11\rangle - a_2|00\rangle + a_3|01\rangle)_{24} + |1111\rangle_{\alpha_1 1\alpha_2 3}(a_0|11\rangle - a_1|10\rangle - a_2|01\rangle + a_3|00\rangle)_{24}
\end{bmatrix} \tag{7}$$

Similarly, if the measurement result for the single particle 11 is $|1\rangle_{11}$, the same measurement results for the four particles $(\alpha_1, 1, \alpha_2, 3)$ can be obtained after the Bell measurements. Now, the QT subsystem, composed of Alice and Bob can be rewritten as

$$|\zeta_3'\rangle =$$

$$\left[\begin{array}{c}
|0000\rangle_{\alpha_1 1\alpha_2 3}(a_0|00\rangle - a_1|01\rangle - a_2|10\rangle + a_3|11\rangle)_{24} + |0001\rangle_{\alpha_1 1\alpha_2 3}(-a_0|01\rangle + a_1|00\rangle + a_2|11\rangle - a_3|10\rangle)_{24} \\
+|0010\rangle_{\alpha_1 1\alpha_2 3}(-a_0|10\rangle + a_1|11\rangle + a_2|00\rangle - a_3|01\rangle)_{24} + |0011\rangle_{\alpha_1 1\alpha_2 3}(a_0|11\rangle - a_1|10\rangle - a_2|01\rangle + a_3|00\rangle)_{24} \\
+|0100\rangle_{\alpha_1 1\alpha_2 3}(a_0|00\rangle + a_1|01\rangle - a_2|10\rangle - a_3|11\rangle)_{24} + |0101\rangle_{\alpha_1 1\alpha_2 3}(-a_0|01\rangle - a_1|00\rangle + a_2|11\rangle + a_3|10\rangle)_{24} \\
+|0110\rangle_{\alpha_1 1\alpha_2 3} - (a_0|10\rangle - a_1|11\rangle + a_2|00\rangle + a_3|01\rangle)_{24} + |0111\rangle_{\alpha_1 1\alpha_2 3}(a_0|11\rangle + a_1|10\rangle - a_2|01\rangle - a_3|00\rangle)_{24} \\
+|1000\rangle_{\alpha_1 1\alpha_2 3}(a_0|00\rangle - a_1|01\rangle + a_2|10\rangle - a_3|11\rangle)_{24} + |1001\rangle_{\alpha_1 1\alpha_2 3}(-a_0|01\rangle + a_1|00\rangle - a_2|11\rangle + a_3|10\rangle)_{24} \\
+|1010\rangle_{\alpha_1 1\alpha_2 3}(-a_0|10\rangle + a_1|11\rangle - a_2|00\rangle + a_3|01\rangle)_{24} + |1011\rangle_{\alpha_1 1\alpha_2 3}(a_0|11\rangle - a_1|10\rangle + a_2|01\rangle - a_3|00\rangle)_{24} \\
+|1100\rangle_{\alpha_1 1\alpha_2 3}(a_0|00\rangle + a_1|01\rangle + a_2|10\rangle + a_3|11\rangle)_{24} + |1101\rangle_{\alpha_1 1\alpha_2 3}(-a_0|01\rangle - a_1|00\rangle - a_2|11\rangle - a_3|10\rangle)_{24} \\
+|1110\rangle_{\alpha_1 1\alpha_2 3}(-a_0|10\rangle - a_1|11\rangle - a_2|00\rangle - a_3|01\rangle)_{24} + |1111\rangle_{\alpha_1 1\alpha_2 3}(a_0|11\rangle + a_1|10\rangle + a_2|01\rangle + a_3|00\rangle)_{24}
\end{array}\right] \tag{8}$$

The relationship between all possible combined measurement results (from TP and Alice) and the corresponding unitary operations applied to particles 2 and 4 to recover $|\varepsilon\rangle$ is provided in Table 1. For instance, if the measurement result of TP is $|1\rangle$ and $(\alpha_1, 1, \alpha_2, 3)$ is $|0010\rangle$, the required unitary operation on particle (2,4) is $ZX \otimes Z$.

Table 1. The relationship between all possible combined measurement results (from TP and Alice) and the corresponding unitary operations applied to particles 2 and 4.

The TP particle	The $\alpha_1, 1, \alpha_2, 3$ particle	Operations to particles 2,4	The TP particle	The $\alpha_1, 1, \alpha_2, 3$ particle	Operations to particles 2,4
0	$\|0000\rangle$	$I \otimes I$	1	$\|0000\rangle$	$Z \otimes Z$
0	$\|0001\rangle$	$I \otimes X$	1	$\|0001\rangle$	$Z \otimes ZX$
0	$\|0010\rangle$	$X \otimes I$	1	$\|0010\rangle$	$ZX \otimes Z$
0	$\|0011\rangle$	$X \otimes X$	1	$\|0011\rangle$	$XZ \otimes XZ$
0	$\|0100\rangle$	$I \otimes Z$	1	$\|0100\rangle$	$Z \otimes I$
0	$\|0101\rangle$	$I \otimes XZ$	1	$\|0101\rangle$	$Z \otimes X$
0	$\|0110\rangle$	$X \otimes Z$	1	$\|0110\rangle$	$XZ \otimes I$
0	$\|0111\rangle$	$X \otimes XZ$	1	$\|0111\rangle$	$XZ \otimes X$
0	$\|1000\rangle$	$Z \otimes I$	1	$\|1000\rangle$	$I \otimes Z$
0	$\|1001\rangle$	$Z \otimes X$	1	$\|1001\rangle$	$I \otimes XZ$
0	$\|1010\rangle$	$XZ \otimes I$	1	$\|1010\rangle$	$X \otimes Z$
0	$\|1011\rangle$	$XZ \otimes X$	1	$\|1011\rangle$	$X \otimes XZ$
0	$\|1100\rangle$	$I \otimes I$	1	$\|1100\rangle$	$Z \otimes Z$
0	$\|1101\rangle$	$Z \otimes XZ$	1	$\|1101\rangle$	$I \otimes X$
0	$\|1110\rangle$	$XZ \otimes Z$	1	$\|1110\rangle$	$X \otimes I$
0	$\|1111\rangle$	$XZ \otimes XZ$	1	$\|1111\rangle$	$X \otimes X$

Meanwhile, the RSP process from Bob to Alice is carried out simultaneously. When the measurement result of TP particle is $|0\rangle_{11}$, a set of mutually orthogonal basis vectors (MOBVs) performed on the particle

pairs (5,8) to obtain amplitude information is given by

$$\begin{aligned}
|\mu_{00}\rangle &= b_0 |00\rangle + b_1 |01\rangle + b_2 |10\rangle + b_3 |11\rangle \\
|\mu_{01}\rangle &= b_1 |00\rangle - b_0 |01\rangle + b_3 |10\rangle - b_2 |11\rangle \\
|\mu_{10}\rangle &= b_2 |00\rangle - b_3 |01\rangle - b_0 |10\rangle + b_1 |11\rangle \\
|\mu_{11}\rangle &= b_3 |00\rangle + b_2 |01\rangle - b_1 |10\rangle - b_0 |11\rangle
\end{aligned} \tag{9}$$

Now the RSP subsystem can be decomposed as

$$\begin{aligned}
|\zeta_4\rangle &= \frac{1}{2} |\mu_{00}\rangle_{58} (b_0 |0000\rangle + b_1 |0101\rangle + b_2 |1010\rangle + b_3 |1111\rangle)_{69710} \\
&+ \frac{1}{2} |\mu_{01}\rangle_{58} (b_0 |0000\rangle - b_1 |0101\rangle + b_2 |1010\rangle - b_3 |1111\rangle)_{69710} \\
&+ \frac{1}{2} |\mu_{10}\rangle_{58} (b_0 |0000\rangle - b_1 |0101\rangle - b_2 |1010\rangle + b_3 |1111\rangle)_{69710} \\
&+ \frac{1}{2} |\mu_{11}\rangle_{58} (b_0 |0000\rangle + b_1 |0101\rangle - b_2 |1010\rangle - b_3 |1111\rangle)_{69710} \\
&= \frac{1}{2} (|\mu_{00}\rangle_{58} + |\mu_{01}\rangle_{58} X_9 \otimes ZX_{10} + |\mu_{10}\rangle_{58} X_6 \otimes (ZX_7 \otimes Z_{10}) + \\
&|\mu_{11}\rangle (X_6 \otimes X_9) \otimes (ZX_7 \otimes X_{10})) (b_0 |0000\rangle + b_1 |0101\rangle + \\
&b_2 |1010\rangle + b_3 |1111\rangle)_{69710}
\end{aligned} \tag{10}$$

Table 2. The relationship between amplitude measurement bases and corresponding operations applied to Bob's particles (6,9) and Alice's particles (7,10).

Amplitude measurement bases	Operations to particles 6,9	Operations to particles 7,10
$\|\mu_{00}\rangle$	$I \otimes I$	$I \otimes I$
$\|\mu_{01}\rangle$	$I \otimes X$	$I \otimes ZX$
$\|\mu_{10}\rangle$	$X \otimes I$	$ZX \otimes Z$
$\|\mu_{11}\rangle$	$X \otimes X$	$ZX \otimes X$

After Bob performs a measurement on the particle pair (5,8), Alice can obtain the amplitude information. She then applies unitary operations on her own particles (7,10) and, depending on the protocol, might also influence Bob's particles (6,9) to recover the state. The relationship between amplitude measurement bases and the corresponding operations is shown in Table 2. For example, if the measurement result of the particle pair (5,8) is $|\mu_{01}\rangle$, Bob applies X to particle 9 and Alice applies ZX to particle 10. After this step, the state of the remaining RSP system becomes $b_0 |0000\rangle + b_1 |0101\rangle + b_2 |1010\rangle + b_3 |1111\rangle$.

To extract the phase information, Bob then measures particles (6,9) using a second set of mutually orthogonal basis vectors, defined as

$$\begin{aligned}
|\varphi'_{00}\rangle &= \frac{1}{2} \left(|00\rangle + e^{-i\lambda_1} |01\rangle + e^{-i\lambda_2} |10\rangle + e^{-i\lambda_3} |11\rangle\right) \\
|\varphi'_{01}\rangle &= \frac{1}{2} \left(|00\rangle - e^{-i\lambda_1} |01\rangle + e^{-i\lambda_2} |10\rangle - e^{-i\lambda_3} |11\rangle\right) \\
|\varphi'_{10}\rangle &= \frac{1}{2} \left(|00\rangle + e^{-i\lambda_1} |01\rangle - e^{-i\lambda_2} |10\rangle - e^{-i\lambda_3} |11\rangle\right) \\
|\varphi'_{11}\rangle &= \frac{1}{2} \left(|00\rangle - e^{-i\lambda_1} |01\rangle - e^{-i\lambda_2} |10\rangle + e^{-i\lambda_3} |11\rangle\right)
\end{aligned} \tag{11}$$

Under the measurement result of the joint projective measurement bases, the state of the remaining

RSP subsystem can be rewritten as

$$\begin{aligned}|\zeta_5\rangle_{69710} = |\varphi'_{00}\rangle_{69} \otimes (I_7 \otimes I_{10}) |\varphi\rangle_{710} + |\varphi'_{01}\rangle_{69} \otimes (I_7 \otimes Z_{10}) |\varphi\rangle_{710} \\ + |\varphi'_{10}\rangle_{69} \otimes (Z_7 \otimes I_{10}) |\varphi\rangle_{710} + |\varphi'_{11}\rangle_{69} \otimes (Z_7 \otimes Z_{10}) |\varphi\rangle_{710}\end{aligned} \tag{12}$$

Table 3. The relationship between phase measurement bases and unitary operations on 7 and 10.

Phase measurement bases	Operations to particles 7,10
$\|\varphi'_{00}\rangle$	$I \otimes I$
$\|\varphi'_{01}\rangle$	$I \otimes Z$
$\|\varphi'_{10}\rangle$	$Z \otimes I$
$\|\varphi'_{11}\rangle$	$Z \otimes Z$

After Alice receives the measurement result sent by Bob, she can obtain the required phase information. Then Alice can perform the corresponding operation to restore the state $|\varphi\rangle$. For example, if the measurement result of the (6,9) particle pair is $|\varphi'_{00}\rangle$, the required operation on Alice is $I_7 \otimes I_{10}$. The other relationship between phase measurement bases and operations to particles 7,10 is shown in Table III.

Moreover, in the case where TP's measurement result is $|1\rangle_{11}$, the initial state of the RSP subsystem after his measurement is different, which can be written as

$$\begin{aligned}|\zeta_4\rangle = \frac{1}{2} (|\mu_{00}\rangle_{58} + |\mu_{01}\rangle_{58} X_9 \otimes ZX_{10} + |\mu_{10}\rangle_{58} X_6 \otimes (ZX_7 \otimes Z_{10}) + \\ |\mu_{11}\rangle (X_6 \otimes X_9) \otimes (ZX_7 \otimes X_{10})) (b_0 |0000\rangle - b_1 |0101\rangle - b_2 |1010\rangle + b_3 |1111\rangle)_{69710}\end{aligned} \tag{13}$$

To bring this state into the same standardized form as in the $|0\rangle$ case, an additional unitary operation, $Z_7 \otimes Z_{10}$, must be applied to particles 7 and 10 at the end of the protocol. After this step, the left RSP subsystem becomes $b_0 |0000\rangle + b_1 |0101\rangle + b_2 |1010\rangle + b_3 |1111\rangle$ as shown in Equation. (10), so the phase measurement procedure is identical to that described above. Therefore, when the TP measurement result is $|1\rangle_{11}$, an additional unitary operation $Z_7 \otimes Z_{10}$ must be applied at the end to recover $|\varphi\rangle$.

By executing the QT and RSP processes in parallel as described above, Alice and Bob successfully exchange their respective two-qubit quantum information, thereby completing the bidirectional hybrid communication protocol.It should be noted that QT and RSP can be performed simultaneously within the quantum communication system. Furthermore, this hybrid bidirectional communication system can also be extended to the cases where both Alice and Bob mutually perform QT or RSP simultaneously. Finally, the system offers improved time efficiency, with the TP particle playing a crucial controlling role.

3. Noise Analysis

In practical quantum communication systems, environmental decoherence inevitably affects the entangled quantum channel, resulting in the degradation of transmission fidelity. Therefore, it is necessary to investigate the robustness of the proposed bidirectional hybrid quantum communication protocol under noisy environments. In this section, three common quantum noise models are considered, namely the amplitude damping (AD) channel, the phase damping (PD) channel, and the depolarizing (DP) channel. The noisy channels are assumed to affect only particles 1,3,7 and 10 held by Alice.The initial entangled

quantum channel can be written as

$$\rho_0 = |\zeta\rangle \langle\zeta| \tag{14}$$

where state $|\zeta\rangle$ is defined in Equation. (1).

In practical quantum communication, network nodes often exhibit physical asymmetry. For instance, central server nodes (TP) or stationary receivers (Bob) can be well-protected using high-grade quantum memories or error-shielding hardware, whereas end-user nodes (Alice) operate in noisier local environments. Therefore, to evaluate the performance lower bound under asymmetric decoherence, we adopt a single-sided noise model where noisy channels independently affect Alice's qubits (1, 3, 7, 10), while decoherence on Bob's qubits, TP's qubit, and ideal classical channels is assumed to be comparatively negligible. This assumption is commonly used in quantum communication literature to evaluate the robustness of protocols against asymmetric noise and provides a lower bound on performance when one side is less protected.

(a)Amplitude Damping Noise Analysis

The amplitude damping channel describes the energy dissipation process caused by spontaneous emission. The Kraus operators of a single-qubit AD channel are given by

$$E_0 = \begin{bmatrix} 1 & 0 \\ 0 & \sqrt{1-\lambda_{AD}} \end{bmatrix}, E_1 = \begin{bmatrix} 0 & \sqrt{\lambda_{AD}} \\ 0 & 0 \end{bmatrix} \tag{15}$$

where $\lambda_{AD}(0 < \lambda_{AD} < 1)$ denotes the decoherence parameter of the AD channel 1,3,7, and 10, the total Kraus operators can be expressed as

$$K_{uvkl} = E_u^{(1)} \otimes E_v^{(3)} \otimes E_k^{(7)} \otimes E_l^{(10)} \tag{16}$$

where $u, v, k, l \in \{0, 1\}$.Thus, the noisy density matrix under the AD channel becomes

$$\rho_{AD} = \sum_{u,v,k,l} K_{uvkl} \rho_0 K_{uvkl}^{\dagger} \tag{17}$$

After completing the QT and RSP procedures, the fidelity between the ideal output state $|\Psi\rangle$ (the state that would be obtained in the noiseless case) and the actual output state ρ_{AD}^{out} is defined as:

$$F_{AD} = \langle\Psi| \rho_{AD}^{out} |\Psi\rangle \tag{18}$$

where $|\Psi\rangle$ denotes the ideal output state without noise.

Under weak decoherence conditions, the dominant contribution originates from the non-decay component $E_0^{\otimes 4}$. Therefore, the fidelity can be approximately simplified as

$$F_{AD} = (1 - \lambda_{AD})^4 \tag{19}$$

This expression indicates that the fidelity decreases monotonically as the decoherence parameter λ_{AD} increases.

(b)Phase Damping Noise Analysis

Phase damping (PD) noise describes the loss of quantum coherence without energy dissipation and mainly affects the phase information encoded in quantum states. Since the proposed hybrid bidirectional communication protocol contains a phase-sensitive remote state preparation (RSP) subsystem, investigating the influence of PD noise is essential for evaluating the robustness of the protocol.

For a single qubit, the Kraus operators corresponding to the PD channel are given by

$$E_0 = \begin{pmatrix} 1 & 0 \\ 0 & \sqrt{1-\lambda_{PD}} \end{pmatrix}, \quad E_1 = \begin{pmatrix} 0 & 0 \\ 0 & \sqrt{\lambda_{PD}} \end{pmatrix}, \tag{20}$$

where $\lambda_{PD}(0 < \lambda_{PD} < 1)$ represents the decoherence parameter of the phase damping channel.

Assuming that the transmitted qubits 1,3,7and 10 are affected independently by the PD noise. Now the the total kraus operatorsl can be expressed as

$$K_{uvkl} = E_u^{(1)} \otimes E_v^{(3)} \otimes E_k^{(7)} \otimes E_l^{(10)} \tag{21}$$

where $u, v, k, l \in \{0, 1\}$.Thus, the noisy density matrix under the PD channel becomes

$$\rho_{PD} = \sum_{u,v,k,l} K_{uvkl} \rho_0 K_{uvkl}^{\dagger} \tag{22}$$

Consequently, the fidelity between the ideal output state $|\Psi\rangle$ and the actual output density matrix ρ_{PD}^{out} is given by

$$F_{PD} = \langle \Psi | \rho_{PD}^{out} | \Psi \rangle \tag{23}$$

To evaluate the overall performance, we integrate over all possible input state configurations. By strictly preserving all diagonal normalization terms and all off-diagonal interference contributions under the 4-qubit single-sided PD noise channel, the exact average fidelity over the entire parameter space of input states is derived as:

$$F_{PD} = \frac{1 + 3(1-\lambda_{PD})^2}{4} \tag{24}$$

From Equation (24), it can be seen that the fidelity decreases gradually as the decoherence parameter increases. Unlike amplitude damping noise, phase damping does not induce energy loss but suppresses the quantum coherence between basis states. Therefore, the RSP subsystem, which strongly depends on phase information, exhibits higher sensitivity to PD noise.

(c)Depolarizing Noise Analysis

The depolarizing channel describes the random occurrence of Pauli errors during quantum transmission. The Kraus operators of a single-qubit depolarizing channel are given by

$$\begin{aligned} E_0 &= \sqrt{1 - \frac{3\lambda_{DP}}{4}} I, \ E_1 = \frac{\sqrt{\lambda_{DP}}}{2} X, \\ E_2 &= \frac{\sqrt{\lambda_{DP}}}{2} Y, \ E_3 = \frac{\sqrt{\lambda_{DP}}}{2} Z \end{aligned} \tag{25}$$

where represents $\lambda_{DP}(0 < \lambda_{DP} < 1)$ the depolarizing probability.

Similarly, the depolarizing noise acts independently on particles 1,3,7 and 10. Therefore, the combined Kraus operators can be written as

$$K_{uvkl} = E_u^{(1)} \otimes E_v^{(3)} \otimes E_k^{(7)} \otimes E_l^{(10)} \tag{26}$$

where $u, v, k, l \in \{0, 1, 2, 3\}$.

The noisy density matrix under the depolarizing channel becomes

$$\rho_{DP} = \sum_{uvkl} K_{uvkl} \rho_0 K_{uvkl}^{\dagger} \tag{27}$$

The total number of combined Kraus operators is therefore 256. After the communication procedure is completed, the exact fidelity under the depolarizing noisy channel can be expressed as

$$F_{DP} = \langle \Psi | \rho_{DP}^{out} | \Psi \rangle \tag{28}$$

Under weak depolarizing noise, the dominant contribution originates from the identity operator. Hence, the fidelity can be approximately simplified as

$$F_{DP} = \left(1 - \frac{3\lambda_{DP}}{4}\right)^4 \tag{29}$$

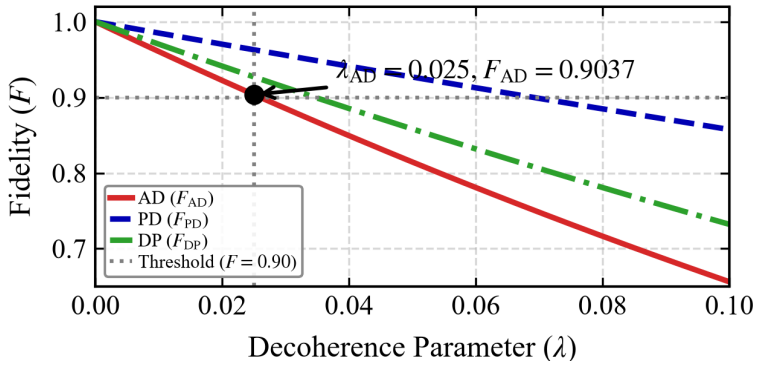


Fig. 2. Variations of average state fidelity under AD, PD, and DP noisy channels with respect to the decoherence parameter λ.

Figure 2 illustrates the average state fidelity F versus the decoherence parameter $\lambda \in [0, 0.10]$ for AD, PD, and DP noise channels. As required by quantum physical constraints, all three fidelity curves start precisely from $F = 1.00$ at $\lambda = 0$.

In summary, our analysis demonstrates that the protocol exhibits distinct robustness under different environmental noise channels. While Phase Damping (PD) noise affects only the phase coherence without causing population relaxation—yielding a remarkably high fidelity of $F_{\mathrm{PD}} \approx 0.9874$ at $\lambda_{PD} = 0.025$—Depolarizing (DP) noise introduces isotropic randomization across all Pauli operators, resulting in $F_{\mathrm{DP}} \approx 0.9270$. Amplitude Damping (AD) noise, which models energy dissipation to the environment, imposes the most stringent limit on transmission fidelity ($F_{\mathrm{AD}} \approx 0.9037$). Consequently, the AD channel serves as the primary bottleneck determining the protocol's practical performance bound. By enforcing an operational noise parameter threshold of $\lambda \leq 0.025$, the state transmission fidelity is rigorously guaranteed to remain above the 90% benchmark under all three noise models simultaneously, confirming the physical feasibility of the proposed scheme in realistic noisy environments.

In addition, the noise analysis reveals that the protocol exhibits asymmetric sensitivity to different types of noise: it is relatively robust against amplitude damping and depolarizing noise in the weak-noise regime, while phase damping has a more pronounced effect on the RSP component due to its phase-sensitive nature. The numerical results indicate that the proposed protocol maintains moderate fidelity under realistic noise conditions, and its performance can be further enhanced by incorporating entanglement purification or quantum error correction codes.

4. Conclusion

The efficiency η of the quantum communication system is typically evaluated using the formula:

$$\eta = \frac{c}{p+q} \tag{30}$$

Here, c represents the number of qubits to be transmitted, p denotes the number of particles in the pre-shared entangled state (i.e., the quantum channel), and q is the number of classical bits consumed, including all classical communication required for measurement outcomes from all parties involved in the protocol.

In this scheme, c=4 corresponds to the two-qubit state teleported from Alice to Bob via QT and the two-qubit state prepared for Alice via RSP. The quantum channel consists of p=11 qubits as defined in Eq. (1). The classical communication cost must account for all measurement results that are necessary for the recovery of the transmitted states.Alice performs two Bell-state measurements on her particle pairs $(\alpha_1, 1)$ and $(\alpha_2, 3)$. As shown in Table 1, there are 16 possible combined measurement outcomes, which require $\log_2 16 = 4$ classical bits to be transmitted from Alice to Bob. Bob performs two sets of joint projective measurements on his pair of particles. The first set on particles (5,8) yields one of four possible outcomes $\{|\mu_{00}\rangle, |\mu_{01}\rangle, |\mu_{10}\rangle, |\mu_{11}\rangle\}$, requiring 2 classical bits. The second set on particles (6,9) yields one of four possible outcomes $\{|\varphi'_{00}\rangle, |\varphi'_{01}\rangle, |\varphi'_{10}\rangle, |\varphi'_{11}\rangle\}$, requiring another 2 classical bits. These 4 bits must be transmitted from Bob to Alice. The third-party controller TP measures particle 11 in the basis $\{|0\rangle_{11}, |1\rangle_{11}\}$. This single-bit result must be sent to both Alice and Bob independently, because Alice needs it to select the correct unitary operations from Table 1 (specifically, whether to use the $|0\rangle$ *or* $|1\rangle$ column), while Bob needs it to determine whether an additional operation $Z_7 \otimes Z_{10}$ is required at the end of the RSP procedure. Therefore, this step contributes 2 classical bits (1 bit to Alice and 1 bit to Bob).

Summing all contributions, the total classical communication cost is

$$q = q_{\text{Alice}\to\text{Bob}} + q_{\text{Bob}\to\text{Alice}} + q_{\text{TP}\to\text{Alice}} + q_{\text{TP}\to\text{Bob}} = 4 + 4 + 1 + 1 = 10. \tag{31}$$

Thus, the efficiency of the proposed protocol is

$$\eta = \frac{4}{11+10} = \frac{4}{21} \approx 19.05\%. \tag{32}$$

Although the inclusion of RSP and the controlled quantum channel leads to a moderate efficiency compared to some simpler bidirectional teleportation schemes, the protocol offers greater versatility. It is

adaptable to a wider range of communication scenarios, as it integrates two different types of quantum information transmission (QT and RSP) within a single framework. Table 4 provides a comparison of several bidirectional quantum communication protocols, where all efficiency values are calculated under their respective original definitions.It should be noted that in Table 4 BQT (2022), proposed by Mafi et al., achieves higher efficiency yet only performs bidirectional quantum teleportation, unlike the scheme in this paper, which simultaneously realizes RSP during QT.

Table 4. Comparison of Four Bidirectional Quantum Communication Protocols.

Scheme	c (qubits transmitted)	p (entangled qubits)	q (classical bits)	η
BQT (2022)(Mafi et al. [14])	2n	—	4n	28%
CBQC(2025)(Yang [33])	3	8	2	21.43%
BQT(2022)(Cao et al. [34])	2	6	2	20%
BAQCT (2015)(Zhang et al. [12])	3	8	1	18.75%
BQOT (2024)(Yuan et al. [16])	2	8	2	12.5%
Proposed Scheme	4	11	10	19.05%

In light of recent progress in versatile quantum teleportation architectures and bidirectional quantum communication protocols [35–37], this paper presents a novel bidirectional hybrid quantum communication protocol for two-qubit states. It enables two parties to simultaneously exchange quantum information through distinct mechanisms: QT for transmitting unknown states and RSP for transmitting known states. Specifically, one party performs a Bell-state measurement on the state to be teleported by applying CNOT and Hadamard (H) gates, while the other party reconstructs the state via a joint projective measurement. Based on the exchanged classical information, both parties implement appropriate unitary operations to recover the desired quantum states.

Furthermore, the proposed scheme can be extended to higher-dimensional systems (e.g., qudits) and can be adapted to symmetric scenarios where both parties perform QT, both perform RSP, or any hybrid combination of the two.

Acknowledgment

This work is supported by the National Science Foundation of China (No. 61873162) and the Key Laboratory of System Control and Information Processing, Ministry of Education, China (No. Scip20240106).

5. References

[1] Bennett C H, Brassard G, Crépeau C, Jozsa R, Peres A and Wootters W K 1993 *Phys. Rev. Lett.* **70** 1895

[2] Bennett C H, DiVincenzo D P, Shor P W, Smolin J A, Terhal B M and Wootters W K 2001 *Phys. Rev. Lett.* **87** 077902

[3] Lo H K 2000 *Phys. Rev. A* **62** 012313

[4] Pati A K 2001 *Phys. Rev. A* **63** 014302

[5] Mahdavipour K, Nosrati F, Sciara S, Lo Franco R and Cangiotti N 2024 *PRX Quantum* **5** 040350

[6] Hu X M, Zhang C, Liu B H, Cai Y, Ye X J, Guo Y, Xu J S, Li C F and Guo G C 2020 *Phys. Rev. Lett.* **125** 230501

[7] Sisodia M 2022 *Int. J. Theor. Phys.* **61** 270

[8] Bao S and Zhang Y 2024 *Int. J. Theor. Phys.* **63** 85

[9] Sun S and Zhang H 2021 *Quantum Inf. Process.* **20** 211

[10] Peng J Y, Yang Z, Tang L and Peng J S 2023 *Quantum Inf. Process.* **22** 141

[11] Zha X W, Zou Z C, Qi J X and Song H Y 2013 *Int. J. Theor. Phys.* **52** 1740

[12] Zhang D, Zha X W, Li W and Yu Y 2015 *Quantum Inf. Process.* **14** 3835

[13] Kazemikhah P, Tabalvandani M B, Mafi Y and Aghababa H 2022 *Int. J. Theor. Phys.* **61** 17

[14] Mafi Y, Kazemikhah P, Ahmadkhaniha A, Tabalvandani M B and Aghababa H 2022 *Opt. Quantum Electron.* **54** 568

[15] Wang M and Li H S 2022 *Quantum Inf. Process.* **21** 44

[16] Yuan H, Liu X Y and Zhang Z J 2024 *Quantum Inf. Process.* **23** 127

[17] Yuan H, Pan G Z, Xue X X and Zhang Z J 2024 *Int. J. Theor. Phys.* **63** 268

[18] Gong L , Chen X B, Xu G and Li Z P 2024 *Adv. Quantum Technol.* **7** 2300183

[19] Verma V 2021 *IEEE Commun. Lett.* **25** 936

[20] Ramachandran M, Balakrishnan S 2022 *Int. J. Theor. Phys.* **61** 127

[21] Yang B C 2025 *J. Appl. Phys.* **138** 184402

[22] Feng Y H, Zhou R G and Zhang X X 2025 *Phys. Scr.* **100** 025104

[23] Bolokian M, Orouji A A and Houshmand M 2023 *Opt. Quantum Electron.* **55** 835

[24] Sisodia M 2022 *Int. J. Theor. Phys.* **61** 90

[25] Cai R, Yu X T and Zhang Z C 2018 *Int. J. Theor. Phys.* **57** 1723

[26] Xu J and Zhou R G 2023 *Quantum Inf. Process.* **22** 376

[27] Kazemikhah P and Aghababa H 2021 *Int. J. Theor. Phys.* **60** 378

[28] Lei H R, Tang J G and Peng J Y 2025 *PLOS ONE* **20** e0332405

[29] Yang B C 2023 *Int. J. Theor. Phys.* **62** 106

[30] Zou X F, Wang X, Rong Z B, Huang Z M, Liu J F and Chen Y 2023 *Int. J. Theor. Phys.* **62** 43

[31] Aisan Y, Maihemuti N, Peng J Y and Tang J G 2025 *Eur. Phys. J. Plus* **140** 506

[32] Zhang X H, Jin W T, Zeng H X, Feng J L and Yang C S 2023 *Int. J. Theor. Phys.* **62** 95

[33] Yang B C 2025 *Laser Phys. Lett.* **22** 065205

[34] Cao Z L, Qi J X and Zhang Y G 2022 *Int. J. Theor. Phys.* **61** 81

[35] Zhang Z H, Zhang Y, Wang Z, et al. 2025 *Chinese Phys. B* **34** 040301

[36] Zhou Y Y, Jia X J, Xie C D, et al. 2024 *Chinese Phys. B* **33** 034209

[37] Gu S P, Ying J W, Wang X F, Zhou L and Sheng Y B 2025 *Chinese Phys. B* **34** 110308